

Parameterization of monoenergetic electron impact ionization

Xiaohua Fang,¹ Cora E. Randall,¹ Dirk Lummerzheim,² Wenbin Wang,³ Gang Lu,³ Stanley C. Solomon,³ and Rudy A. Frahm⁴

Received 5 September 2010; revised 12 October 2010; accepted 18 October 2010; published 24 November 2010.

[1] We report a new parameterization of ionization in the Earth's atmosphere by isotropically precipitating monoenergetic (100 eV to 1 MeV) electrons. This new parameterization is the first one based on sophisticated first-principle models, and represents a significant improvement in accuracy, particularly for incident auroral and lower energies. Without previous need to interpolate over source energy and atmospheric range, the new parameterization provides an easier implementation with a robust fit of model calculations for a wide range of incident energies and atmospheric conditions. By decomposing any incident energy spectrum into contiguous monoenergetic components and then calculating and integrating their resulting ionization, our parameterization is a valuable tool that can be used in conjunction with global models to accurately quantify the impact from realistic precipitating electrons during space weather events. **Citation:** Fang, X., C. E. Randall, D. Lummerzheim, W. Wang, G. Lu, S. C. Solomon, and R. A. Frahm (2010), Parameterization of monoenergetic electron impact ionization, *Geophys. Res. Lett.*, 37, L22106, doi:10.1029/2010GL045406.

1. Introduction

[2] Numerous models have been developed to study the interaction between energetic charged particles and the Earth's atmosphere (cf. Solomon [2001, and references therein] for electrons; Fang *et al.* [2004, 2005, and references therein] for protons). However, physics-based model calculations of the energy degradation and angular scattering processes are too time-consuming to be included in large-scale computations, even with modern supercomputers. For efficient computation in global ionosphere/atmosphere models, particle impact ionization calculations must be parameterized so that ionization rate altitude profiles can be quickly determined.

[3] A few parameterizations exist for simplifying calculation of electron impact ionization, such as Spencer [1959], Lazarev [1967], Roble and Ridley [1987], and Fang *et al.* [2008, hereafter F08]. The latter two were developed for incident electrons in a Maxwellian energy distribution. However, in-situ spectral measurements usually exhibit a non-Maxwellian feature with a high- or low-energy tail [e.g., Frahm *et al.*, 1997]. Moreover, cases were reported where

incident monoenergetic electrons were superposed on relatively smooth background precipitation [Rees, 1969]. As illustrated later in section 4, severe errors can be introduced in ionization calculations by approximating particle precipitation using prescribed functions. Therefore, a straightforward and more accurate strategy is to decompose any incident spectra into contiguous monoenergetic beams, apply a parameterization to calculate the ionization from individual components, and finally sum their results.

[4] While the parameterizations by Spencer [1959] and Lazarev [1967] are for monoenergetic electrons, their energy dissipation is based on vertically incident particles with a zero pitch angle. In-situ measurements reveal that precipitation is generally isotropic in pitch angle. To reflect reality, adjustments were added by Lummerzheim [1992] to extend the Spencer [1959] method for several prescribed (including isotropic) angular distributions. The adjusted Spencer-Lummerzheim parameterization (hereinafter referred to as SL59) was subsequently adopted in satellite data analyses by Winningham *et al.* [1993] and Sharber *et al.* [1996]. The SL59 method was further modified above 1 keV to include the energy deposited by bremsstrahlung X-rays as done by Frahm *et al.* [1997]; however, that underlying parameterization method of ionization from monoenergetic and isotropically incident electrons is essentially that of SL59. A major limitation of all the existing parameterizations (except F08) is that they were derived from range calculations, which simply involves scaling laboratory measurements to the atmosphere. Due to the lack of detailed collisional processes, the accuracy of range calculations is limited, particularly at low energies. The goal of this work is to employ much more accurate first-principle models to parameterize ionization from monoenergetic and isotropically incident electrons.

2. First-Principle Ionization Computation

[5] We apply two first-principle models to solve Boltzmann transport equations and calculate the resulting ionization for parameterization. Isotropically incident monoenergetic electrons with energies ranging from 100 eV to 1 MeV are considered, representing most precipitating particles of magnetospheric origin. The background atmosphere is specified using the MSIS-90 empirical model [Hedin, 1991] with various parameters.

[6] The transport of precipitating monoenergetic ($E_{\text{mono}} < 50$ keV) electrons and resulting ionization rates are simulated using a multi-stream model [Lummerzheim *et al.*, 1989; Lummerzheim and Liliensten, 1994]. This energy limit is dictated by the maximum energy grid setting in the multi-stream codes. For higher incident energies (at which angular scattering becomes less significant), we apply the two-stream model of Solomon *et al.* [1988] and Solomon and Abreu [1989]. The two-stream model results are further multi-

¹Laboratory for Atmospheric and Space Physics, University of Colorado at Boulder, Boulder, Colorado, USA.

²Geophysical Institute, University of Alaska Fairbanks, Fairbanks, Alaska, USA.

³High Altitude Observatory, National Center for Atmospheric Research, Boulder, Colorado, USA.

⁴Southwest Research Institute, San Antonio, Texas, USA.

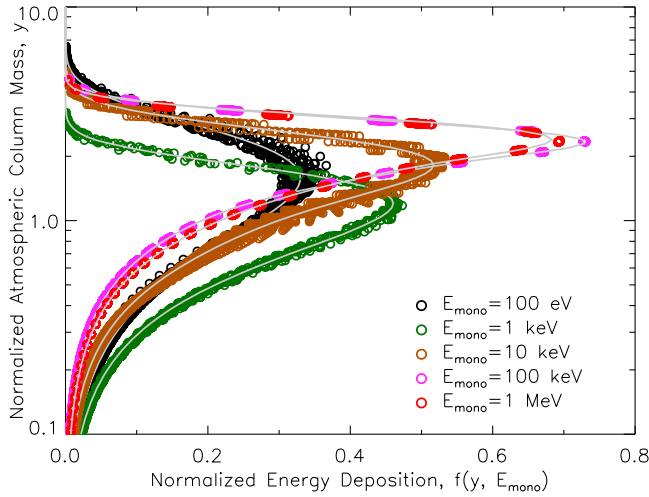


Figure 1. Normalized energy deposition versus normalized atmospheric column mass for five representative precipitating electron energies. Results are shown for a set of 42 different model atmospheres (circles). The parameterization is derived to fit the averaged atmospheric effects (gray curves).

plied by a small scaling factor (varying from 1.09 to 1.16, depending on incident energy and background atmosphere), so that the mean energy loss per ion pair production is 35 eV in accordance with laboratory measurements [Rees, 1989]. This 35-eV rule of thumb is accurate for precipitating high-energy electrons but not for low-energy particles (cf. F08). In both models, secondary electron effects have been included. Good agreement at 50 keV ensures continuity of the two model results. Note that the ionization from generated bremsstrahlung X-rays is not considered, which may be significant only below 50 km altitude [Frahm *et al.*, 1997], and can be estimated from a separate parameterization model [e.g., Berger *et al.*, 1974].

3. Parameterization

[7] The first-principle model results are transformed into normalized quantities before curve fitting. We adopt the basic procedures that were first proposed by Roble and Ridley [1987] and further improved by F08 for incident Maxwellian distributions. Appropriate modifications are applied to account for proper normalization for monoenergetic distributions. This is part of achieving our goal to derive a parameterization for use in large-scale computations rather than to develop a new physics-based model.

[8] The first quantity is normalized atmospheric column mass (y) as a function of vertical location (z):

$$y = \frac{2}{E_{\text{mono}}} \left(\frac{\rho(z)H(z)}{6 \times 10^{-6}} \right)^{0.7}, \quad (1)$$

where E_{mono} is incident electron energy (keV), ρ is the atmospheric mass density (g cm^{-3}), and H is the scale height (cm):

$$H(z) = \frac{kT(z)}{m(z)g(z)}, \quad (2)$$

where k is the Boltzmann constant, T is the atmospheric temperature, m is the average molecular weight, and g is the gravitational acceleration.

[9] The second normalized quantity is energy dissipation (f):

$$f = q_{\text{tot}}(z) / \left(\frac{Q_{\text{mono}}}{\Delta\epsilon} \frac{1}{H(z)} \right), \quad (3)$$

where q_{tot} is the total ionization rate ($\text{cm}^{-3} \text{s}^{-1}$), Q_{mono} is the incident electron energy flux ($\text{keV cm}^{-2} \text{s}^{-1}$), and $\Delta\epsilon$ is a constant of 0.035 keV.

[10] Figure 1 shows the numerical model results in terms of the two normalized quantities. The sensitivity of the results to atmospheric conditions is examined for a total of 42 MSIS-90 model atmospheres by changing both the $F_{10.7}$ (from 50 to 300 by a step of 50) and A_p values (from 5 to 65 by a step of 10). It is found that the ionization rate dependence on atmospheric conditions is negligible after the quantities are normalized, similar to the findings of F08. To a reasonable approximation, our parameterization is derived to fit the averaged atmospheric effects.

[11] Following the energy-dependent parameterization scheme introduced by F08, we fit the first-principle model results with a 2-D least squares analysis,

$$f(y, E_{\text{mono}}) = C_1 y^{C_2} \exp(-C_3 y^{C_4}) + C_5 y^{C_6} \exp(-C_7 y^{C_8}), \quad (4)$$

where each coefficient C_i ($i = 1, \dots, 8$) is separately dependent on incident energy by the exponential of a third-order polynomial with coefficients P_{ij}

$$C_i(E_{\text{mono}}) = \exp \left(\sum_{j=0}^3 P_{ij} \cdot (\ln(E_{\text{mono}}))^j \right), \quad (5)$$

where $\ln(E_{\text{mono}})$ is the natural logarithm. The fitting process iteratively adjusts 32 parameters (i.e., P_{ij} , $i = 1, \dots, 8$, $j = 0, \dots, 3$) to minimize the chi square. These best fit parameters are given in Table 1. Application of the new parameterization requires the following steps:

- [12] 1. Calculate the C_i coefficients using equation (5) and Table 1.
- [13] 2. Calculate the y values throughout the atmosphere using equation (1).
- [14] 3. Calculate the normalized energy dissipation f values using equation (4).
- [15] 4. Obtain the altitude profile of q_{tot} by substituting the f values into equation (3).

4. Verification and Discussion

[16] The first-principle models have been extensively validated in comparisons with in-situ measurements [e.g.,

Table 1. Parameterization Coefficients P_{ij} for Isotropically Incident Monoenergetic 100 eV to 1 MeV Electrons

P_{ij}	$j = 0$	$j = 1$	$j = 2$	$j = 3$
$i = 1$	1.2461E+0	1.4590E+0	-2.4226E-1	5.9545E-2
$i = 2$	2.2397E+0	-4.2291E-7	1.3645E-2	2.5333E-3
$i = 3$	1.4175E+0	1.4459E-1	1.7043E-2	6.3971E-4
$i = 4$	2.4877E-1	-1.5089E-1	6.3089E-9	1.2370E-3
$i = 5$	-4.6511E-1	-1.0508E-1	-8.9570E-2	1.2245E-2
$i = 6$	3.8601E-1	1.7543E-3	-7.4296E-4	4.6088E-4
$i = 7$	-6.4545E-1	8.4955E-2	-4.2858E-2	-2.9930E-3
$i = 8$	9.4893E-1	1.9738E-1	-2.5066E-3	-2.0693E-3

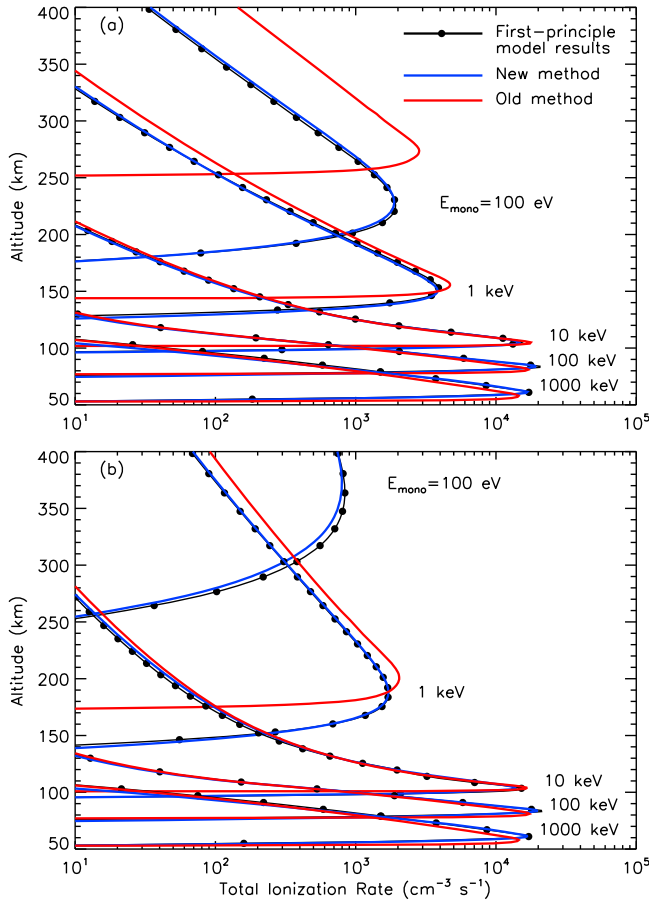


Figure 2. Comparison of ionization rate altitude profiles obtained from the first-principle models, our new parameterization method, and the old SL59 method. The comparison is made for five representative precipitating electron energies, and in two MSIS atmospheres with (a) $F_{10.7} = 50$, $A_p = 5$, and (b) $F_{10.7} = 300$, $A_p = 65$, respectively. The total incident energy of electrons is $1 \text{ erg cm}^{-2} \text{ s}^{-1}$. In the second atmosphere for $E_{\text{mono}} = 100 \text{ eV}$, ionization from the old method occurs at altitudes higher than 400 km.

Lummerzheim et al., 1989], laboratory experiments [e.g., Lummerzheim and Lilensten, 1994], and more sophisticated Monte Carlo calculations [Solomon, 2001]. Therefore, the validity of our new parameterization can be tested by simply comparing to these models. Figure 2 compares the ionization results obtained from the first-principle models to those from our new parameterization and the SL59 method. Our parameterization achieves remarkable agreement with those given by the sophisticated but time-consuming numerical models. The agreement persists when the incident energy varies over four orders of magnitude from 100 eV to 1 MeV, and in both geomagnetic quiet and disturbed atmospheric conditions. In contrast, the previous parameterization provides fairly good results only at relatively high energies. For auroral and lower energy ($\sim 1 \text{ keV}$) electron precipitation, the SL59 parameterization does not yield reliable results compared to detailed first-principle model calculations. This is consistent with what is expected for range calculations, given that many simplified assumptions are made, such as continuous energy loss and no angular scattering during particle transport. To convert energy dissipation into ioni-

zation, a constant mean energy loss per ion pair production is adopted regardless of incident energy, introducing additional errors in range calculations (cf. F08). These become unrealistic, particularly for low energy electrons.

[17] Together, Figures 1 and 2 suggest that the ionization rate dependence on atmospheric conditions can be reasonably neglected when the results are normalized. Figure 3 summarizes results for extensive tests including more incident energies and more atmospheric conditions by varying days of the year and locations (in addition to $F_{10.7}$ and A_p indices) in the MSIS model. Four days of the year are selected for evaluation: spring/fall equinoxes and summer/winter solstices. The geographic location is also varied in terms of longitude (0° , 90° , 180° , 270°) and latitude (60° , 70° , 80°). As a result, the comparison is systematically undertaken in a total of 2016 background atmospheres. Figure 3 includes the mean values and standard deviations of the errors when monoenergetic electrons interact with these various atmospheres. It is seen that our new method reliably reproduces the numerical model results for various atmospheric conditions over a wide precipitating energy range. The errors in the ionization peak altitude are less than 5 km for most comparisons. The rising errors in the peak location at low energies are partially due to the fact that the peak ionization region becomes broader as energy decreases (see Figure 2). The errors in the total ionization rate and the peak intensity generally fall well within $\pm 5\%$ and

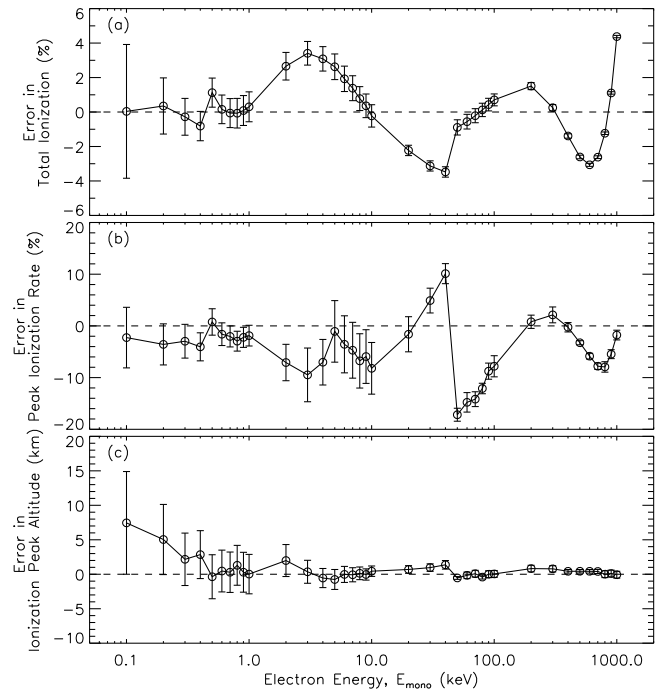


Figure 3. Errors in ionization rate altitude profiles derived from our parameterization. Errors are calculated by comparing numerical model results to our parameterization results for (a) total ionization rates, (b) peak ionization intensities, and (c) ionization peak altitudes. For each precipitating electron energy, the errors are calculated for a set of 2016 different MSIS atmospheres. Open circles indicate mean errors and error bars denote one standard deviation from the mean values.

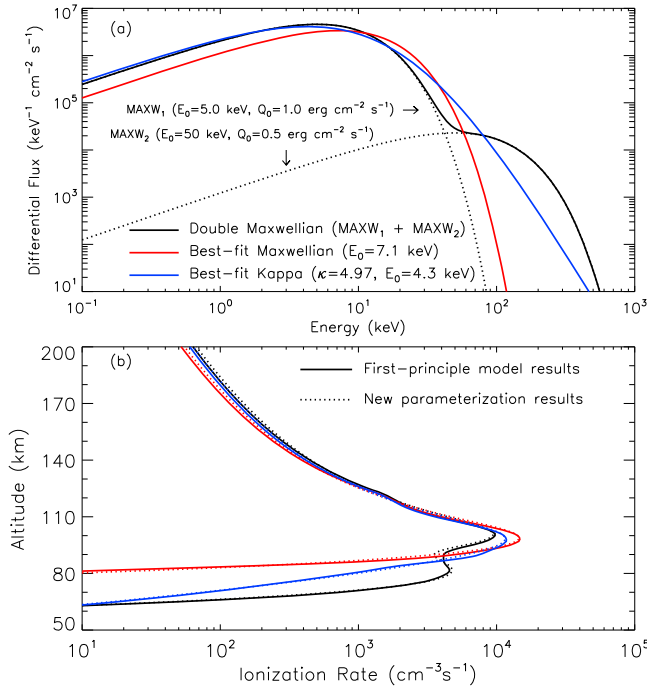


Figure 4. (a) Example of Maxwellian and κ fits to a double-Maxwellian energy spectrum. (b) Corresponding ionization rates when energy spectra are applied at the top of the atmosphere.

$\pm 10\%$, respectively. The peak ionization rates predicted by our parameterization have slightly higher errors at around $E_{\text{mono}} = 50$ keV. This is because of the small discrepancy between the multi-stream and two-stream models, which are employed to deal with < 50 keV and ≥ 50 keV electron precipitation, respectively. However, the integrated energy flux at ~ 50 keV usually represents only a small part of the total energy, so the larger errors are generally of only minor importance. For precipitating energy spectra in reality, the error in peak ionization is expected to be less than 5%.

[18] Figure 4 shows an application to complex electron precipitation. As an example, incident particles are assumed to have a double-Maxwellian distribution [e.g., Codrescu *et al.*, 1997], with components coming from different source regions (e.g., plasma sheet and ring current). Two commonly used functions are employed to fit the differential number fluxes (cm⁻² s⁻¹ keV⁻¹), under the same total number and energy fluxes as the original spectrum. The Maxwellian and κ functions are defined, respectively, by

$$\phi_M(E) = \frac{Q_0}{2E_0^3} E \exp\left(-\frac{E}{E_0}\right), \quad (6)$$

$$\phi_\kappa(E) = \frac{Q_0}{2E_0^3} \frac{(\kappa-1)(\kappa-2)}{\kappa^2} E \left(1 + \frac{E}{\kappa E_0}\right)^{-\kappa-1}, \quad (7)$$

where Q_0 is the total energy flux (keV cm⁻² s⁻¹) and E_0 is the characteristic energy (keV). While the κ function provides a relatively better fit to the high-energy tail, comparisons of ionization calculations clearly show that

both spectral approximations result in considerable errors (up to orders of magnitude). Here the spectra are divided into logarithmic energy bins at fine resolution, and the ionization is obtained by integrating the contributions of individual monoenergetic components. Directly utilizing satellite spectral measurements instead of spectral approximations is feasible with the new parameterization because of its accuracy and numerical efficiency. As demonstrated in Figure 4b, results from our parameterization are nearly indistinguishable from the first-principle model calculations at all altitudes, regardless of incident spectral shapes. Moreover, without having to interpolate over source energy and atmospheric range like in the SL59 method, ours provides an easier implementation and faster computation.

5. Conclusion

[19] We have parameterized the altitude profiles of ionization rates in the Earth's atmosphere by precipitating monoenergetic electrons in an isotropic angular distribution. This is the first parameterization that is derived by fitting to first-principle model results. The extensive error analysis shows that our parameterization achieves a robust fit for input energies from 100 eV to 1 MeV, and high accuracy is preserved under various atmospheric conditions. In contrast, the existing parameterization method, which was based on the range calculation technique, does not yield reliable results for incident auroral and lower energies (i.e., ≤ 1 keV). Since the majority of kinetic energy is carried by auroral electrons, this work represents a significant improvement over previous methods.

[20] In large-scale computations, it is often assumed that precipitating particles have prescribed energy distributions. However, severe errors can be caused by spectral approximations. With our new parameterization, such practice is no longer necessary. Any energy spectrum can be reconstructed by a superposition of contiguous monoenergetic distributions, and the total ionization can be obtained by accumulating the contributions of individual components. Our accurate and fast computation algorithm removes the need for offline calculations, and allows self-consistent simulation of particle impact and feedback. This is particularly desirable in the study of magnetosphere-ionosphere-atmosphere coupling via particle precipitation during space weather events.

[21] **Acknowledgments.** The work was supported by NASA grants NNX09AI04G and NNX06AC05G. NCAR is sponsored by NSF.

References

- Berger, M. J., S. M. Seltzer, and K. Maeda (1974), Some new results on electron transport in the atmosphere, *J. Atmos. Terr. Phys.*, **36**, 591.
- Codrescu, M. V., T. J. Fuller-Rowell, R. G. Roble, and D. S. Evans (1997), Medium energy particle precipitation influences on the mesosphere and lower thermosphere, *J. Geophys. Res.*, **102**, 19,977.
- Fang, X., M. W. Liemohn, J. U. Kozyra, and S. C. Solomon (2004), Quantification of the spreading effect of auroral proton precipitation, *J. Geophys. Res.*, **109**, A04309, doi:10.1029/2003JA010119.
- Fang, X., M. W. Liemohn, J. U. Kozyra, and S. C. Solomon (2005), Study of the proton arc spreading effect on primary ionization rates, *J. Geophys. Res.*, **110**, A07302, doi:10.1029/2004JA010915.
- Fang, X., C. E. Randall, D. Lummertzheim, S. C. Solomon, M. J. Mills, D. R. Marsh, C. H. Jackman, W. Wang, and G. Lu (2008), Electron impact ionization: A new parameterization for 100 eV to 1 MeV electrons, *J. Geophys. Res.*, **113**, A09311, doi:10.1029/2008JA013384.
- Frahm, R. A., J. D. Winningham, J. R. Sharber, R. Link, G. Crowley, E. E. Gaines, D. L. Chenette, B. J. Anderson, and T. A. Potemra (1997), The

- diffuse aurora: A significant source of ionization in the middle atmosphere, *J. Geophys. Res.*, **102**, 28,203.
- Hedin, A. E. (1991), Extension of the MSIS thermosphere model into the middle and lower atmosphere, *J. Geophys. Res.*, **96**, 1159.
- Lazarev, V. I. (1967), Absorption of the energy of an electron beam in the upper atmosphere, *Geomagn. Aeron.*, **7**, 219.
- Lummerzheim, D. (1992), Comparison of energy dissipation functions for high energy auroral electrons and ion precipitation, *Rep. UAG-R-318*, Geophys. Inst., Univ. of Alaska Fairbanks, Fairbanks.
- Lummerzheim, D., and J. Liliensten (1994), Electron transport and energy degradation in the ionosphere: Evaluation of the numerical solution, comparison with laboratory experiments and auroral observations, *Ann. Geophys.*, **12**, 1039.
- Lummerzheim, D., M. H. Rees, and H. R. Anderson (1989), Angular dependent transport of auroral electrons in the upper atmosphere, *Planet. Space Sci.*, **37**, 109.
- Rees, M. H. (1969), Auroral electrons, *Space Sci. Rev.*, **10**, 413.
- Rees, M. H. (1989), *Physics and Chemistry of the Upper Atmosphere*, Cambridge Univ. Press, New York.
- Roble, R. G., and E. C. Ridley (1987), An auroral model for the NCAR thermospheric general circulation model (TGCM), *Ann. Geophys.*, **5A**, 369.
- Sharber, J. R., R. Link, R. A. Frahm, J. D. Winningham, D. Lummerzheim, M. H. Rees, D. L. Chenette, and E. E. Gaines (1996), Validation of UARS particle environment monitor electron energy deposition, *J. Geophys. Res.*, **101**, 9571, doi:10.1029/95JD02702.
- Solomon, S. C. (2001), Auroral particle transport using Monte Carlo and hybrid methods, *J. Geophys. Res.*, **106**, 107.
- Solomon, S. C., and V. J. Abreu (1989), The 630 nm dayglow, *J. Geophys. Res.*, **94**, 6817.
- Solomon, S. C., P. B. Hays, and V. J. Abreu (1988), The auroral 6300 Å emission: Observations and modeling, *J. Geophys. Res.*, **93**, 9867.
- Spencer, L. V. (1959), *Energy Dissipation by Fast Electrons*, NBS Monogr., **1**, 70 pp.
- Winningham, J. D., et al. (1993), The UARS particle environment monitor, *J. Geophys. Res.*, **98**, 10,649.
- X. Fang and C. E. Randall, Laboratory for Atmospheric and Space Physics, University of Colorado, 392 UCB, Boulder, CO 80309-0392, USA. (xiaohua.fang@lasp.colorado.edu)
- R. A. Frahm, Southwest Research Institute, 6220 Culebra Rd., PO Drawer 28510, San Antonio, TX 78228, USA.
- G. Lu, S. C. Solomon, and W. Wang, High Altitude Observatory, National Center for Atmospheric Research, 3080 Center Grn., Boulder, CO 80301, USA.
- D. Lummerzheim, Geophysical Institute, University of Alaska Fairbanks, PO Box 757320, Fairbanks, AK 99775-7320, USA.